

AD736018

Microwave Laboratory
W. W. Hansen Laboratories of Physics
Stanford University
Stanford, California

DEVELOPMENT OF CHALCOPYRITE CRYSTALS FOR
NONLINEAR OPTICAL APPLICATIONS

Interim Technical Report No. 5

for

Contract F33615-70-C-1640

for the period

1 August - 31 October 1971

M. I. Report No. 2024

November 1971

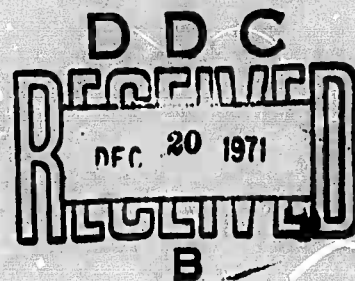
Sponsored by
Advanced Research Projects Agency
ARPA Order No. 1636

Reproduced by
**NATIONAL TECHNICAL
INFORMATION SERVICE**
Springfield, Va. 22151

Prepared for

Air Force Materials Laboratory
Wright-Patterson Air Force Base, Ohio

Distribution of this
document is unlimited.



DISTRIBUTION STATEMENT A
Approved for public release;
Distribution Unlimited

DISCLAIMER NOTICE

THIS DOCUMENT IS THE BEST
QUALITY AVAILABLE.

COPY FURNISHED CONTAINED
A SIGNIFICANT NUMBER OF
PAGES WHICH DO NOT
REPRODUCE LEGIBLY.

Contractor: The Board of Trustees of the Leland Stanford Jr. University

Contract No. F33615-70-C-1640

ARPA Order Number 1636

Program Code Number OD10

Effective Date of Contract: 1 August 1970

Contract Expiration Date: 31 July 1972

Amount of Contract: \$60,000

Corresponsible Investigators: S.E.Harris and R.L. Byer - (415) 327-7800

Project Engineer: V. L. Donlan, AFML/LPE

Distribution of this
document is unlimited.

I. INTRODUCTION

During the first year, the chalcopyrite growth effort was directed at a single compound, CdGeAs_2 . The potential applications of this crystal in nonlinear optics is now fully evaluated. It promises to be a very useful nonlinear material providing that there is sufficient improvement in crystal quality. Past crystal growth has been by the Bridgman-Stockbarger technique. We are now preparing to grow crystals by the Czochralski method.

Recently we have started growth of a new chalcopyrite compound CdGeP_2 , another potentially very useful nonlinear crystal. The choice of CdGeP_2 was made after a study of all the II-IV-V₂ chalcopyrites, estimating the optical properties from the measured properties of the III-V analogs. The results of this study are included in Appendix I.

II. CRYSTAL GROWTH

A. CdGeAs_2

(1) Bridgman-Stockbarger

The last series of boules have been grown from stoichiometric melt. The 0.5 - 1.0 weight percent excess As used previously does not improve the optical transmission. We also use slower growth rates ($\sim 4^\circ/\text{hr}$) and larger gradients ($\sim 34^\circ/\text{cm}$). The growth gives fairly consistent results from boule to boule and we are planning impurity doping to investigate the effects on crystal properties such as resistivity, optical transmission, and index homogeneity. The orientation of large single crystal regions in a boule is usually with the chalcopyrite unit cell [111] direction within 10° of the boule axis. This agrees with the literature which reports the [111] direction as the fastest growth direction for the chalcopyrites.

There is a correlation between grain boundaries and crystal cracking. Large single crystal regions have usually few cracks. We therefore hope that the cracking problem may be solved with the growth of large homogeneous single crystals. The cracking might also be related to the constraints imposed by the walls of the quartz crucible. We are now measuring the thermal expansion coefficient and its anisotropy to gain some further insight.

For the last boule B6, the synthesis and the growth were done in one step. Previously the synthesizing was done as a separate step. This had the disadvantage that there was some vapor in the crucible which deposited on the walls when the synthesized material was quenched. It

was impossible to retrieve this deposit. The one step process assures that no material is lost. However, we are faced with the problem of obtaining uniform mixing and achieving fully reacted material in the crucible as well as in the capillary before the growth starts. The first run showed incomplete mixing. An ultrasonic vibrator has been constructed to aid the mixing process in succeeding runs.

(ii) Czochralski

At present, initial experiments are being carried out to determine the correct growth conditions. In addition, a furnace is being assembled.

B. CdGeP_2

To date two boules have been grown. The CdP_2 is synthesized first and then reacted with Ge to form CdGeP_2 . The fully reacted material is then used to grow single crystals by the Bridgman-Stockbarger technique similar to the growth of CdGeAs_2 . Due to observed Si vitrification, a carbon crucible is used to synthesize the CdGeP_2 . The first boules have single crystal regions of approximately 1 mm^3 and they show the same cracking pattern as observed for CdGeAs_2 .

A good etch for CdGeP_2 is 10% Br_2 solution in ethyl alcohol. This reveals grain boundaries and twin lines after etching for about 15 sec.

III. IMPURITY ANALYSIS OF CdGeAs_2

Table I shows the results of an impurity analysis of three slices from boule #33. The slices were from different sections of the boule and they had different resistivity and optical transmission. The impurity analysis was performed by the Bell and Howell Electronic Materials Division in Pasadena using spark source mass spectrometry. There appears to be very little correlation between the impurity analysis and the optical transmission. A possible explanation is that only a small fraction of the boule cross section was probed and homogeneity problems may have obscured the results. The probed area was less than one mm^2 and only a few tenths of a milligram was analyzed. The unusually large oxygen and carbon concentrations are most probably due to hydrocarbons and possibly an oxide layer on the surface.

TABLE I
IMPURITY CONCENTRATIONS IN STANFORD CADMIUM GERMANIUM ARSENIDE
(IN PARTS PER MILLION ATOMIC)

Element ^(a)	Detection Limit ^(b)	Opaque	Max T = 20%	Max T = 5%
Li	0.007	0.012	0.083	0.017
C	0.03	4.6-25	3,200 (75-10,000)	19
N	0.03	0.18	0.51	0.28
O	0.03	76	900	3,600
F	0.07	0.27	0.48	0.22
Na	0.01	0.35	8.3	0.73
Mg	0.3	N.D.	0.49	N.D.
Al	0.1	0.37	3.9	0.80
Si	1	6.7	N.D.	N.D.
S	0.03	1.5	1.1	4.5
K	0.01	0.052	0.51 (6.6*)	0.19
Ca	0.03	0.065	0.25 (3.3*)	0.074

(a) No analysis was made for hydrogen. Analyses for gold are not given since the samples were sparked against high purity gold counterelectrodes. Background lines of the matrix interfere with the analyses for Cl, Mn, and Fe. Other impurities not listed were not detected and have concentrations less than 0.3 ppma.

(b) Determined for 3×10^{-7} coulomb exposure.

* Seen on one exposure only.

N.D. Not detected.

IV. ELECTRON PROBE MICROANALYSIS

We have completed an extensive microprobe analysis of several boules to investigate possible deviations from stoichiometric composition. The absolute accuracy of microprobe measurements are between 2 and 5 weight percent. For absolute calibration we use Cd, CdS, Ge, and GaAs as standards and determine the weight fraction W_u of the elements in the unknown (CdGeAs_2) using the expression

$$W_u = W_s \frac{F_s}{F_u} \frac{I_s}{I_u}, \quad (1)$$

where W_s is the weight fraction of the element in the standard, I_s and I_u are the X ray intensities from the standard and the unknown, and F_s and F_u corrects for the matrix absorption in the standard and the unknown. We have determined F_s/F_u from tables in Birks¹ for an accelerating voltage of 25 kV, electrons incident at 62.5° , and a takeoff angle ψ of 38.5° . Table II gives the product $W_s F_s/F_u$.

The relative accuracy of the microprobe analysis can be as good as a few tenths of one percent. Table III lists some experimental results for CdGeAs_2 . Within the experimental error excess As does not perturb the stoichiometric composition. The results confirm what we would expect from our previous phase diagram studies, that CdGeAs_2 exists only in a narrow homogeneity region.

We have also studied carefully an etched boule cross section containing several grains, some optical transparent and some opaque. No variation in stoichiometry or irregularities at the grain boundaries could be observed within the experimental resolution.

TABLE II

MAGNITUDE OF $W_s F_s / F_u$ FOR MICROPROBE ANALYSIS OF CdGeAs_2

Standard	$\text{Cd}_{L\alpha}$	$\text{Ge}_{K\alpha}$	$\text{As}_{K\alpha}$
Cd	115.26		
CdS	82.23		
Ge		101.99	
GaAs			49.37

TABLE III
MICROPROBE ANALYSIS OF CdGeAs_2

Boule number	W_{Cd}	W_{Ge}	W_{As}	Growth condition	Optical transmission
16	31.33	22.21	46.46	0.5 Wt % excess As	opaque
26A (top of boule)	31.33	22.12	46.55	Stoichiometric	Max 40%
26C	31.34	22.29	46.36	Stoichiometric	Max 15%
31	31.64	22.03	46.34	0.5 Wt % excess As	Max 10%
33	31.38	22.36	46.26	0.5 Wt % excess As	Max 25%
CdGeAs_2	33.57	21.68	44.75	—	—

V. OPTICAL MEASUREMENTS

A. CdGeAs₂

We have determined the type I phasematching angle for doubling CO₂ using a 1.95 mm crystal from boule #31. When the crystal is mounted normal to the laser beam, back reflections make the laser unstable. By motor scanning the crystal through the unstability and phasematching positions we can determine the phasematching angle very accurately with respect to the crystal front surface. The measured phasematching angle is $31.7^\circ \pm 0.5^\circ$, while the index of refraction data from boule #16 gives a calculated angle of 35.6° . The measured full width of the external angle at the half-power point was 5.9° in good agreement with an angle of 6° that we calculate using the expression

$$\Delta\theta_{\text{ext}} = \frac{\lambda}{2.25 \ell \tan \rho} \quad (2)$$

with $\ell = 1.95$ mm and $\rho = 0.02313$ rad.

Since the walk-off angle limits the maximum useful interaction length, the most attractive parametric oscillator construction would be a 90° phasematched oscillator with a tunable pump. Figure 1 shows the tuning curve for such a device. The tunable pump may be a LiNbO₃ or LiIO₃ parametric oscillator.

B. CdGeP₂

We have not yet obtained sufficiently large single crystals to measure the indices of refraction by the prism method. Boule #1 had

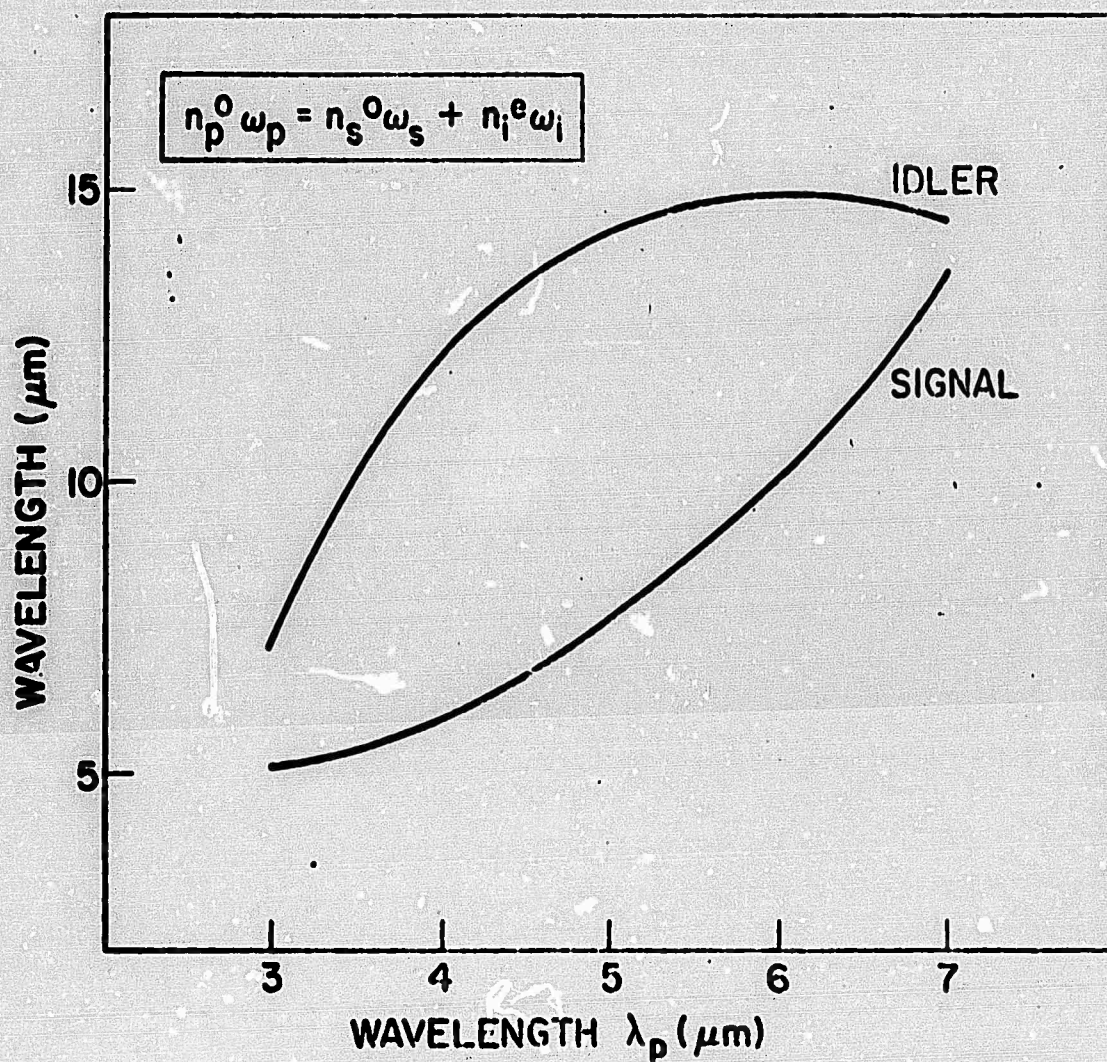


Figure 1--Theoretical tuning curves for CdGeAs_2 for 90° phasematching.

a small transparent section which could be studied under an infrared microscope. The measured transmission range is between 7500 \AA and $13 \text{ }\mu\text{m}$ with the reststrahl frequency located at approximately $26 \text{ }\mu\text{m}$. By probing with a CO_2 laser beam we measured the transmission through the most transparent sections to be at least 30% for a 0.5 mm thick sample.

VI. ELECTRICAL MEASUREMENTS

A. CdGeAs₂

We have experimented with ohmic contacts. Indium soldered contact works well down to at least 77°K. Some crystals of approximately 1 × 2 × 7 mm have been cut for Hall effect measurements.

B. CdGeP₂

The first boule was n-type with a resistivity of approximately $10^4 - 10^5 \Omega\text{cm}$.

REFERENCES

1. L. S. Birks, Electron Probe Microanalysis (Interscience Publications, New York, 1963).

APPENDIX I

ESTIMATION OF THE OPTICAL PROPERTIES
OF THE II-IV-V₂ CHALCOPYRITE COMPOUNDS

ESTIMATION OF THE OPTICAL PROPERTIES
OF THE II-IV-V₂ CHALCOPYRITE COMPOUNDS*

by

H. Kildal and R. L. Byer

Microwave Laboratory
Stanford University
Stanford, California

ABSTRACT

Several of the II-IV-V₂ chalcopyrite compounds are attractive for nonlinear optical applications. In order to evaluate their potential, their optical parameters are determined using the close resemblance to the III-V analogs and their relative anisotropic bond polarizability which has been measured for a few of the chalcopyrites.

*This research was supported by the Advanced Research Projects Agency of the Department of Defense and was monitored by the Air Force Materials Laboratory MAYE, under contract #F33516-70-C-1640.

ESTIMATION OF THE OPTICAL PROPERTIES
OF THE II-IV-V₂ CHALCOPYRITE COMPOUNDS

by

H. Kildal and R. L. Byer

Microwave Laboratory
Stanford University
Stanford, California

The II-IV-V₂ compounds with a chalcopyrite structure have recently generated considerable interest as new infrared nonlinear crystals.^{1,2} The nonlinear coefficients are large and compare with the III-V compounds and the chalcopyrites have the necessary birefringence for phasematching. The chalcopyrite point group symmetry is $\bar{4}2m$ which allows both type I and type II phasematching.² Unfortunately, the growth of high optical quality material presents problems and for best progress it seems reasonable to concentrate on a few compounds. In choosing which compounds to grow, the important considerations are transmission range, birefringence, and magnitude of the nonlinear coefficients. However, measured values exist only for a few of the chalcopyrites, and a method to estimate their properties would be very useful. We outline a procedure using the close resemblance between the II-IV-V₂ compounds and their III-V analogs. The predicted properties agree well with the few measured experimental values. By a different method using Levine's bond charge model,^{3,4} Chemla⁵ has also estimated the indices of refraction and Miller's delta⁶ for the chalcopyrites.

Table I lists the properties of the III-V compounds used to estimate the properties of the chalcopyrites in Table II. The optical bandgap

TABLE I
OPTICAL PROPERTIES OF III-V COMPOUNDS

	Unit cell volume [Å ³]	Reststrahl frequency ^(a) [μm]	Index of refraction ^(a)	Nonlinear coefficient rel. GaAs ^(b)
AlP	162.0	~ 15.6	2.95	.58
GaP	162.0	25	2.95	
InP	202.1	28.5	3.1	
AlAs	181.5		3.2	1.00
GaAs	180.7	34	3.3	
InAs	222.4	41.1	3.5	
				2.22

(a) R. K. Willardson and A. C. Beer, Semiconductors and Semimetals, vol. 3: Optical Properties of III-V Compounds (Academic Press, New York, 1967).

(b) J. J. Wynne and N. Bloembergen, Phys. Rev. 188, 1211 (1969).

TABLE II
ESTIMATED OPTICAL PROPERTIES OF THE CHALCOPYRITES

	ZnSIP ₂	ZnGeP ₂	ZnSnP ₂	CdSIP ₂	CdGeP ₂	CdSnP ₂	ZnSIA ₂	ZnGeAs ₂	ZnSnAs ₂	CdSIA ₂	CdGeAs ₂	CdSnAs ₂
III-V analogs	GaP+AlP	GaP	GaP+InP	InP+AlP	InP+GaP	InP	GaAs+AlAs	GaAs	GaAs+InAs	InAs+AlAs	InAs+GaAs	InAs
Melting point (°C)	1370 ^(a)	1025 ^(b)	~950 ^(b)	~1120 ^(b)	~790 ^(a)	~670 ^(c)	~1090 ^(a)	~880 ^(a)	~775 ^(d)	~950 ^(a)	670 ^(a)	595 ^(d)
Unit cell volume (Å ³)	304.5	321.7	350.7	336.3	355.1	400.9	342.5	353.8	400.7	376.8	335.1	442.7
Tetragonal compression ^(a) $\epsilon = 2 - \frac{c}{a}$.065	.029	.000	.163	.123	.048	.061	.034	.000	.151	.112	.044
$\epsilon = 4\pi \cdot j(f)$.076	.056	-.044	-.172	.132	.044	-.080	.056	-.044	-.164	.144	.044
Measured Reststrahl frequency (μm)	18.7 ^(a)		27.2 ^(h)			23 ⁽¹⁾					36.5 ^(j)	
Estimated Reststrahl frequency (μm)		25	26.5	19.4	26.5	29.0		34	37.3		37.3	41.1
Expected transmission range (μm)	.54 ^(a) - .9	.56 ^(a) - .12	.36 ^(h) - .13	.55 ^(a) - .9	.72 ⁽¹⁾ - .13	1.1 ⁽ⁿ⁾ - .14	.53 ⁽ⁿ⁾	1.5 ^(a) - .17	1.9 ^(a) - .18	.35 ^(a)	2.3 ^(a) - .18	4.5 ^(a) - .20
Measured ϵ_{av}	3.1 ^(a)	3.1 ^(p)	2.8 ^(h)		3.7 ^(q)	3.3 ⁽¹⁾			3.6 ^(r)	3.6 ^(s)	3.6 ^(t)	
Estimated ϵ_{av}	3.03	2.95	3.05	3.15	3.07	3.11	3.33	3.31	3.42	3.40	3.44	3.51
Measured birefringence $\epsilon_e - \epsilon_o$.05 ^(a)	.038 ^(p)			.11 ^(q)	.04 ⁽ⁿ⁾					.095 ^(s)	.16 ^(t)
Estimated birefringence $\epsilon_e - \epsilon_o$.05	.04	-.02	.14	.11	.04	.05	.03	-.02	.11	.095	.03
Measured nonlinear coefficient rel. GaAs		.83									3.4	
Estimated nonlinear coefficient rel. GaAs		.6						1.0	1.7		1.7	2.2
Estimated nonlinear coefficient from Miller's δ	.6	.5	.6	.7	.6	.7	1.1	1.0	1.3	1.4	1.3	1.5

(a) Handbook of Chemistry and Physics, 51st edition.

(b) S. A. Mughal, A. J. Payne, B. Ray, J. of Materials Science 4, 835 (1969).

(c) E. Buehler, J. H. Wernick, and J. L. Shay (private communication).

(d) D. B. Gasson, P. J. Holmes, I. C. Jennings, B. R. Marathe, and J. E. Parrott, J. Phys. Chem. Solids 21, 1291 (1962).

(e) G. K. Averkieva, N. A. Goryunova, V. D. Proshukhan, and M. Serginoy, Sov. Phys. Doklady 15, 385 (1970).

- (f) R. C. Smith (private communication).
- (g) I. P. Kasilov, E. Buehler, and J. H. Wernick, *Phys. Rev. B* **2**, 960 (1970).
- (h) L. B. Zlatkin, J. F. Markov, A. I. Stekhanov, and M. S. Shur, *Phys. Stat. Sol.* **22**, 473 (1969).
- (i) L. B. Zlatkin, Yu. F. Marlov, V. M. Orlov, V. I. Sokolova, and M. S. Shur, *Sov. Phys. - Semiconductors* **5**, 1181 (1971).
- (j) L. B. Zlatkin, Yu. F. Markov, A. I. Stekhanov, and M. S. Shur, *J. Phys. Chem. Solids* **31**, 567 (1970).
- (k) L. B. Zlatkin, E. K. Ivanov, and O. P. Startsev, *Phys. Stat. Sol. (a)* **1**, 661 (1970).
- (l) J. L. Shay, E. Buehler, and J. H. Wernick, "Electroreflectance Absorption Coefficient, and Energy Band Structure of CdTeF_2 near the Direct Energy Gap," to be published.
- (m) J. L. Shay and E. Buehler, *Phys. Rev. Letters* **26**, 506 (1971).
- (n) J. L. Shay, E. Buehler, and J. H. Wernick, *Phys. Rev. B* **3**, 2004 (1971).
- (o) J. L. Shay and E. Buehler, *Phys. Rev. B* **3**, 2598 (1971).
- (p) G. D. Boyd, E. Buehler, and F. G. Storz, *Appl. Phys. Letters* **18**, 301 (1971).
- (q) N. A. Goryunova, L. B. Zlatkin, and E. K. Ivanov, *J. Phys. Chem. Solids* **31**, 2557 (1970).
- (r) N. A. Goryunova, B. N. Marlov, V. D. Frochukhan, and M. Serginov, *Phys. Stat. Sol. (a)* **2**, K249 (1970).
- (s) R. L. Byer, M. Kildal, and R. S. Feigelson, "CdTeAs₂ - A New Nonlinear Crystal Phase-matched at 10.6 μm ," to be published in *Appl. Phys. Letters*.
- (t) R. K. Karymshakov, Yu. I. Urzhanov, and Yu. V. Shnartsev, *Sov. Phys. - Semiconductors* **5**, 1702 (1971).

frequency and two phonon absorption determine the transmission range of the chalcopyrites. In CdGeAs_2 , i.e., the two phonon absorption at room temperature is about 20 cm^{-1} . The three phonon absorption is much weaker and is approximately 0.4 cm^{-1} . We take the two phonon absorption frequency to be half the reststrahl frequency. For the reststrahl frequency ω_r we use the experimental value or an estimate from the reststrahl frequencies ω_a and ω_b of the III-V analogs using the relation

$$\omega_r = \frac{1}{2} \sqrt{\omega_a^2 + \omega_b^2} \quad (1)$$

By assigning bond polarizabilities to the II-V and the III-V bonds, we derive expressions for the indices of refraction and for the birefringence by summing over the thirty-two bonds within the chalcopyrite unit cell. With a linear polarizability tensor $\vec{\alpha}$ and a second order polarizability tensor $\vec{\beta}$, we write the induced polarization of a bond as

$$\vec{p}(t) = \epsilon_0 \vec{\alpha} \cdot \vec{E}(t) + \vec{\beta} : \vec{E}(t) \vec{E}(t) \quad (2)$$

We assume uniaxial bond symmetry and write the transverse and the longitudinal linear bond polarizabilities as α_\perp and α_\parallel . Defining an average bond polarizability as $\alpha = \frac{1}{3}(2\alpha_\perp + \alpha_\parallel)$ and the anisotropy as $\gamma = (\alpha_\parallel - \alpha_\perp)$, we follow Chemla and obtain for the susceptibility

tensor that

$$\bar{\chi} = \bar{\epsilon} - 1 = \frac{16}{V}(\alpha_{AC} + \alpha_{BC})\mathbb{I} + \frac{16}{9V}[\gamma_{AC}(\tau + \sigma) + \gamma_{BC}(\tau - \sigma)] \begin{pmatrix} 1 & 0 & 0 \\ 0 & 1 & 0 \\ 0 & 0 & -2 \end{pmatrix}, \quad (3)$$

where AC and BC denote the two different bonds and V is the unit cell volume. The parameters τ and σ characterize the chalcopyrite structure. Since the II and IV cations have different covalent radii, the anion is not exactly in the center of the cation tetrahedra. It is positioned a distance $a(x - \frac{1}{4})$ off the center closer to the cations with the smallest radii.⁷ With the lattice parameters a and c we have $\tau = 2 - c/a$ for the tetragonal compression and $\sigma = 4x - 1$. In Eq. (3) BC denotes the bond to the smallest cation. Assuming the bond polarizability is approximately the same as for the III-V analogs, we have for the average susceptibility of the chalcopyrites that

$$\chi_{av} = \frac{V_a}{V} \chi_a + \frac{V_b}{V} \chi_b, \quad (4)$$

where V_a and V_b are the unit cell volume of the III-V analogs and χ_a and χ_b are the measured susceptibilities. The average estimated index in Table II agrees well with experimental values.

For the relative birefringence we obtain from Eq. (3) that

$$\frac{\Delta n}{n} = \frac{n_e - n_o}{n} = \frac{\chi_e - \chi_o}{2(1 + \chi_{av})} = - \frac{\gamma_a(\tau + \sigma) + \gamma_b(\tau - \sigma)}{6(\alpha_a + \alpha_b)}, \quad (5)$$

since χ_{av} is always much greater than one. For the II-IV-V₂ compounds, τ and σ have about the same magnitude so we can approximate Eq. (5)

by

$$\frac{\Delta n}{n} \approx -\frac{1}{6} \frac{\gamma_a}{\alpha_a + \alpha_b} (\tau + \sigma) \quad (6)$$

The maximum positive birefringence occurs when $\alpha_{\perp} \gg \alpha_{\parallel}$. This gives

$$\left(\frac{\Delta n}{n}\right)_{\max} = +\frac{1}{4} \frac{\tau + \sigma}{1 + \alpha_{\perp b} / \alpha_{\perp a}} \quad (7)$$

Trustworthy measurements of the birefringence exist only for a few of the chalcopyrites. Figure 1 shows a plot of the relative birefringence versus $\tau + \sigma$. According to Eq. (6) the birefringence depends mainly on the anisotropic polarizability of the AC bond. Consequently, since A is the cation with the largest radius, the birefringence of ZnSiP_2 and ZnGeP_2 should be determined mainly by the anisotropic polarizability of the ZnP bond. This is confirmed by a linear dependence in Fig. 1. Figure 1 also indicates approximately the same relative anisotropic bond polarizability for the Zn and Cd bonds to the same anion. This needs to be confirmed, however, by more experimental points for the As compounds. In Table II we estimate the birefringence using $\Delta n/n = K(\tau + \sigma)$ with K equal to 0.14 for the P compounds and 0.10 for the As compounds.

Degenerate parametric oscillators or second harmonic generation (SHG) require the largest birefringence. The phasematching angle for SHG is approximately given by

$$\sin \theta_I \approx \sqrt{n/B} \quad (8)$$

for type I phasematching and

$$\sin \theta_{II} \approx \sqrt{2D/B} \quad (9)$$

for type II, where $B = n_e - n_o$ is the birefringence and $D = n_o^{2\omega} - n_o^\omega$ is the dispersion. For type II phasematching the necessary birefringence is approximately 0.6 to 0.7 for 90° phasematching. For propagation at angles less than 90° to the c-axis the walkoff angle limits the effective crystal length l_{\max} for the nonlinear interaction. For confocal focusing we have

$$l_{\max} \approx \frac{\lambda}{2np^2} \quad (10)$$

with the walkoff angle $p \approx -\frac{B}{n} \sin 2\theta$. A crystal with a large birefringence, e.g. 0.1 for CdGeAs_2 , is phasematchable for parametric interaction and second harmonic generation over most of its transparency range. Maximizing the nonlinear interaction, however, requires a crystal with a smaller birefringence to ensure phasematching closer to 90° .

The chalcopyrites have only one independent nonlinear coefficient since $d_{14} = d_{36}$ according to the Kleinman symmetry condition.⁸ Assuming the second order bond polarizability β_{ijk} satisfies the overall permutation symmetry, we express the nonlinear coefficient for the chalcopyrites as^{5,9}

$$d_{14} = d_{xyz} = \frac{8}{V} \frac{1}{3\sqrt{3}} \left[(\beta_{\parallel} - 3\beta_{\perp})_{AC} + (\beta_{\parallel} - 3\beta_{\perp})_{BC} \right], \quad (11)$$

where $\beta_{\parallel} = \beta_{333}$ and $\beta_{\perp} = \frac{1}{2}(\beta_{113} + \beta_{223})$ are the longitudinal and the transverse second order bond polarizabilities. For the III-V compounds, Flytzanis and Ducuing⁹ state that the main contribution to the nonlinear coefficient is from β_{\parallel} , even though the linear polarizability tensor is almost isotropic with a_{\parallel} slightly larger than a_{\perp} . Chemla's calculations for the chalcopyrites include only β_{\parallel} . This approximation may not be valid since the transverse component of the linear polarizability tensor is larger than the longitudinal component. However, we shall make the same approximation so that we may use the measured nonlinear coefficients for the III-V analogs to estimate the nonlinear coefficients for the chalcopyrites using the expression

$$d_{14} = \frac{v_a}{v} (d_{14})_a + \frac{v_b}{v} (d_{14})_b \quad (12)$$

Table II also lists the nonlinear coefficients calculated from $d_{14} = \delta(X_{av})^3$, assuming the Miller's δ is the same for all the chalcopyrites. This assumption is probably true within a factor of two for most chalcopyrites.¹⁰

It follows from Table II that all the chalcopyrites have roughly the same figure of merit d^2/n^3 . Therefore, for nonlinear optics applications it is more important to consider transmission range, birefringence, and crystal quality. The transparency region sets an upper limit for the tuning range of a parametric oscillator. At a fixed idler frequency the gain of a parametric oscillator varies linearly proportional to the pump frequency for walkoff limited interaction lengths.¹¹ It is therefore advantageous to use the shortest pump wavelength permitted

by the bandgap and phasematching condition. An attractive pump source for infrared parametric oscillators is the Nd^{3+} :YAG laser in cases where the bandgap cutoff is shorter than one micron. The nonlinear crystal then also has applications in infrared up-conversion schemes for low noise signal processing¹² or image up-conversion.¹³ Materials with bandgaps shorter than a micron are also attractive from a crystal growth point of view since this allows visual detection of crystal imperfections.

In conclusion we have estimated the optical properties of the II-IV-V₂ compounds based on the analogous III-V compounds. The estimated birefringence and transparency range agrees very well with the few values that have been measured. Several of the chalcopyrites have potential for nonlinear optics applications. The values listed in Table II should assist in the selection of the crystal most suited for a particular application.

REFERENCES

1. G. D. Boyd, E. Buehler, and F. G. Storz, Appl. Phys. Letters 18, 301 (1971).
2. R. L. Byer, H. Kildal, and R. S. Feigelson, Appl. Phys. Letters 19, 237 (1971).
3. B. F. Levine, Phys. Rev. Letters 22, 787 (1969).
4. B. F. Levine, Phys. Rev. Letters 25, 440 (1970).
5. D. S. Chemla, Phys. Rev. Letters 26, 1411 (1971).
6. R. C. Miller, Appl. Phys. Letters 5, 17 (1964).
7. H. Pfister, Acta Cryst. 11, 221 (1958).
8. D. A. Kleinman, Phys. Rev. 126 1977 (1962).
9. Chr. Flytzanis and J. Ducuing, Phys. Rev. 178, 1218 (1969).
10. J. J. Wynne and N. Bloembergen, Phys. Rev. 188, 1211 (1969).
11. S. E. Harris, Proc. IEEE 57, 2096 (1969).
12. D. A. Kleinman and G. D. Boyd, J. Appl. Phys. 40, 546 (1969).
13. R. A. Andrews, IEEE J. Quant. Elect. QE-6, 68 (1970).

FIGURE CAPTIONS

Figure 1. Relative birefringence of the chalcopyrites.

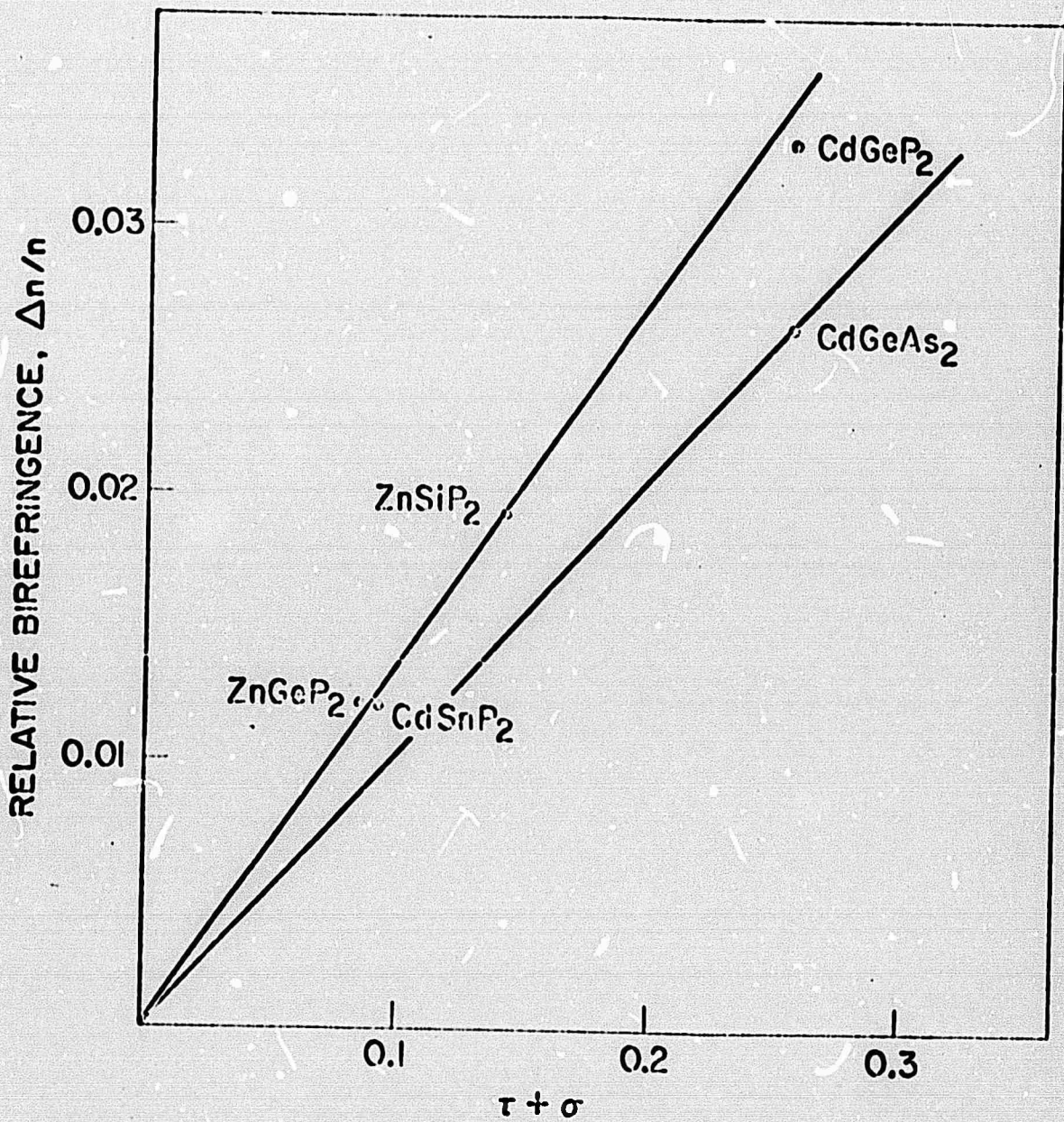


Figure 1